TRANSIENT THERMAL ANALYSIS IN SUBSEA PIPELINES

Jhoany Jhordann Barrera Escobedo
Departamento de Engenharia Mecânica, PUC-RIO, 22453-900, RJ
barrera@mec.puc-rio.br

Angela Ourivio Nieckele
Departamento de Engenharia Mecânica, PUC-RIO, 22453-900, RJ
nieckele@mec.puc-rio.br

Luis Fernando Alzuguir Azevedo
Departamento de Engenharia Mecânica, PUC-RIO, 22453-900, RJ
lfaa@mec.puc-rio.br

Abstract*. Subsea pipelines are employed not only for production but also for transportation. In both situations, warm oil loses heat to the cold sea water. The heat loss to the ambient is controlled by means of thermal insulation, which is designed for steady state operations. During shutdowns, the stagnant fluid in the pipeline loses heat to the cold surrounding, eventually reaching some critical temperature. As a result, several problems can occur, such as formation of hydrates or deposition of high molecular weight paraffins on the inner wall of the subsea line, which can lead to flow line blockage and production shutdown. Re-start of very viscous fluid after shutdown is also critical, since viscosity increases significantly with the reduction of the temperature. This work presents an analysis of the influence of the pipe wall thermal capacitance on the transient behavior of heavily insulated lines. The heat loss from the pipeline is determined, by solving the transient heat conduction equation for the pipewall layers, utilizing a simple one-dimensional model in the radial direction. Results were obtained considering and neglecting the thermal capacitance to evaluate the potential to reach critical temperatures. Comparison with the prediction of commercial softwares was performed. It was shown that accounting for the thermal capacity of the wall is relevant to the determination of cooldown times.*

Key words: *thermal model, transient, cooldown, hydrate formation, paraffin deposition.*

1. Introduction

As drilling and production operations expand into deepwater environments, seawater temperature decreases to a few degrees above freezing, generating a variety of problems, such as hydrate formation in well bores, subsea pipelines and subsea equipment during both drilling and production operations. In pipelines, hydrates can restrict and even block the flow. Partial blockages can have adverse effects including reduced production. Hydrates are crystalline solids formed from a combination of water and one or more hydrocarbon gases such as methane, ethane, or propane which are stable at high pressure and low temperatures, predominant conditions in deepwater operations. In physical appearance, hydrates resemble packed snow or ice. Controlling heat losses is usually the best choice for preventing hydrate formation. Heat losses can be controlled by burying non insulated pipes (Loch, 2000), using insulated flowlines (Denniel & Blair, 2004) or heated flowlines (Cerqueira et al, 2004). Often the temperature in the flowline will be above the hydrate formation in steady state operating conditions. However, during a shutdown or interruption in flow, stagnant fluid in the pipeline loses heat to the surrounding and cools to local seabed temperatures increasing the risk of forming hydrates. Thermal insulation is necessary in these cases to keep the produced fluids above the hydrate temperature long enough for the operator to introduce hydrate inhibitors or until flow can be reestablished. Typically, operators require eight to twelve hours of temperature levels above the hydrate formation temperature at no-flow conditions (Dwight J. et al, 2004).

Wax deposition in production and transportation pipelines is another relevant problem in offshore operations. The crude oil flows out of the reservoir at, typically, 60 ^{o}C into the production pipelines. These lines carry the oil to the platforms and from the platforms to shore. At large water depths, the ocean temperature at the bottom is of the order of 5 ^{o}C. The solubility of wax in the oil is a decreasing function of temperature. As the oil flows, it loses heat to the surrounding water. If the crude oil temperature falls below the Wax Appearance Temperature (WAT), the wax may precipitate and deposit along the inner walls of the pipeline. The accumulation of the deposited material may lead to increased pumping power, decreased flow rate or even to the total blockage of the line with loss of production and capital investment. Again thermal insulation is necessary to avoid the wax precipitation. In order to assure the flow of oil at the desired rates, accurate prediction of the temporal and spatial distributions of the flow inside the pipeline is essential.

Re-start of very viscous fluid after shutdown is also critical in transportation pipelines, since viscosity increases significantly with the reduction of the temperature, requiring excessive pumping power to re-start the flow. Further, low-vapor-pressure fluids can produce column separation problems due pressure losses induced by heat transfer during shut downs (Chiu and Thakur, 1991).

The revision of some commercial flow simulation softwares reveals that a majority of them also carry out thermal calculations. The *Pipeline Studio (TLNET)* software performs the thermal simulation calculating an overall heat transfer coefficient based on equivalent thermal resistances, which is recommended only for steady state regime. In the case of the thermal transient forecast, a determination of the overall heat transfer coefficient is not sufficient, requiring the knowledge of additional thermal properties besides the thermal conductivity, such as density and heat capacity.

The commercial software *OLGA* was developed to solve multiphase and single phase flows. It allows the user to select two distinct conditions to analyze a thermal problem. With the first option, the thermal capacitance of pipe layers is neglected and an overall heat transfer coefficient must be prescribed. The second option, called 3D Thermal module, takes into account the thermal capacitance of the pipe layers. It solves the thermal transient in two steps: in the first step the energy equation is solved for the fluid and pipe wall, yielding the temperature profile of both, the fluid and the pipe wall along the pipeline. In the next step a 2D conduction equation is solved for the solid media surrounding the pipe, giving the temperature distribution over the cross-section along the pipeline. A combination of the solutions of steps one and two result in a 3D temperature field.

The *TRANSTHERMAL* mode of the *Stoner Pipeline Simulator* allows the determination of temperature field inside the pipeline, the pipe-wall, and each pipe wrapping material. The mass, momentum and energy equations are solved for the fluid employing an axial 1D formulation, while a radial 1D conduction equation is solved for the pipe-wall and insulating material.

A literature survey shows few papers dealing with transient thermal analysis. Brown et al (1996) developed a computational model to describe transient heat transfer in pipeline bundles; this model is coupled to the transient, multiphase flow simulator *OLGA*. Walls and insulation are not explicitly accounted for in the bundle model, the thermal resistances of insulations and walls are handled through the use of equivalent heat transfer coefficients. This approach neglects the effects of the thermal capacity of the insulation and walls during transients. The lines containing the multiphase production fluids are modeled by *OLGA*, and the heat transfer between the internal lines, carrier pipe and surrounding is handled by the bundle model. Zabaras and Zhang (1998) present a heat transfer calculation developed as an approximation to the finite elements solution to perform the steady state and transient cooldown analysis for different bundle and pipe-in-pipe configurations. Danielsen and Brown (1999) developed two models to predict the behavior of pipeline bundles, the first one is similar to the above model, the second model is an analytic approach, and according to the authors is not grid sensitive, extremely fast and easy to set up.

The aim of the present paper is the study of the transient cooldown behavior after a system shutdown. To this end, an analysis of the heat transfer through the wall is carried out. The solutions obtained with the models developed in this work are compared with the commercial softwares *OLGA, Stoner* and *TLNET*. The main concern is to address the importance of the energy stored in the insulation layers.

2. Mathematical Modeling

The present model couples the solution of the flow field inside the pipeline and the conduction equation at the pipe wall and insulation. The wall temperature is calculated taking into account the full thermal capacitance of the pipe wall by performing a calculation of the radial temperature distribution, within the pipe wall, which may be made up of several layers of different materials. Heat flow is modeled by radial conduction only; longitudinal conduction within the pipe wall, as well as inside the pipeline, is ignored. Heat transfer between the pipe and the fluid is dependent on the flow characteristics inside the pipe and is determined from convective heat transfer correlations. A convective boundary condition is also specified at the outside boundary, determining the heat flow from the pipe to the ambient.

The flow field inside the pipeline is determined by the solution of the continuity, momentum and energy equations, assuming that the fluid is Newtonian. The flow is uniform along the cross section, and the duct centerline can be inclined with the horizontal direction at an angle α. Due to very high pressure variations, its effect in the pipe deformation is considered. The mass conservation equation can be written as (Wylie and Streeter, 1978)

$$\frac{\partial P}{\partial t} + V\frac{\partial P}{\partial x} + \frac{\rho a^2}{\xi}\frac{\partial V}{\partial x}x + \frac{\rho a^2}{\xi}\frac{V}{A}\frac{\partial A}{\partial x} - \frac{\rho a^2 \beta}{\xi}\frac{\partial T}{\partial t} - \frac{\rho a^2 \beta}{\xi}V\frac{\partial T}{\partial x} = 0 \tag{1}$$

where V, p, T are the velocity, pressure and temperature, respectively. The fluid properties are: density ρ, speed of sound a, coefficient of thermal expansion β. ξ is given by $\xi = 1 + \rho\, a^2\, 2\, C_D\, (D/D_{ref})$ where D and D_{ref} are the pipeline diameter and the reference diameter determined at atmospheric pressure p_{atm}. The pipe deformation due to pressure is accounted by the coefficient C_D, given by $C_D = (1-\nu^2)\, D_{ref} / (2\, e\, E)$, where e is the pipe wall thickness, E the Young's modulus of elasticity of the pipe material, and ν the Poisson's ratio A is the cross section area.

The linear momentum equation can be written as

$$\frac{\partial V}{\partial t} + V\,\frac{\partial V}{\partial x} = -\frac{1}{\rho}\frac{\partial p}{\partial x} - \frac{f}{2}\frac{|V|V}{D} - g\,\sin\alpha \tag{2}$$

where g is gravity and f the hydrodynamic friction coefficient factor, which depends on the Reynolds number

Re = $\rho\ |V|\ D/\mu_f$, where μ_f is the absolute viscosity. In the turbulent regime the friction factor is also a function of the relative pipe roughness ε/D. To simplify the solution, the friction factor is approximated by its fully developed expression. For a laminar regime, **Re** < 2000, it is specified as f= 64/**Re**. For the turbulent regime, **Re** > 2500, the friction factor is approximated by Miller's correlation (Fox and McDonald, 2001), $f = 0.25\ \{\ \log\ [(\varepsilon/D)/3.7+5.74/\mathbf{Re}^{0.9}]\}^{-2}$. Between **Re**= 2000 and 2500, it was assumed a linear variation of the friction factor with the Reynolds number.

The energy conservation equation can be written as

$$\frac{\partial T}{\partial t}+V\frac{\partial T}{\partial x}=\frac{\beta\, T}{\rho\, c_p}\left[\frac{\partial p}{\partial t}+V\frac{\partial p}{\partial x}\right]+\frac{f}{2\, c_p}\frac{V^2|V|}{D}-\frac{4\, U_e}{\rho\, c_p\, D}\left(T-T_{ref}\right) \tag{3}$$

where c_p is the specific heat at constant pressure, U_e is a heat transfer coefficient and T_{ref} is a reference temperature which can be determined according to the approaches called Model 1 and Model 2 that will next be described.

For both models, the inner heat transfer coefficient is computed during the solution of the flow field, as a function of flow regime, flow properties (Prandtl number, $\mathbf{Pr}=\mu_f\, c_p\,/k$) and flow velocities (Reynolds number, **Re**). Both forced and natural convection are considered. The forced convection is evaluated assuming fully developed flow for both laminar and turbulent regimes. For laminar flow (**Re**<2000), the Nusselt number is defined as **Nu**=3.66 corresponding to a constant surface temperature condition. A limiting Reynolds number equal to 10^{-4} is defined to neglect convection, and an equivalent Nusselt number (**Nu** =2) due only to conduction is prescribed.

For turbulent regime, a correlation due to Gnielinski (Incropera and DeWitt, 1998) is utilized

$$\mathbf{Nu}=h_{in}\ D/k=\mathbf{Pr}\,(f/8)\,(\mathbf{Re}\ -\ 1000)/\,[1+12.7\,\sqrt{(f/8)}\ (\mathbf{Pr}^{2/3}-1)]. \tag{4}$$

This correlation is valid for 0.5 < **Pr** < 2000 and 2300 < **Re** < 5×10^6. For the transition zone (2000 < Re < 2500) a linear profile is utilized, **Nu** = 0.01056 **Re** - 17.46). To consider the effects of natural convection, the Nusselt Number is approximated by the Olivier's correlation (Holman, 1983)

$$\mathbf{Nu}=1.75(\mu_m/\mu_w)^{0.14}\left[\mathbf{Re\ Pr}\,(D/L)+0.0083(\mathbf{Gr\ Pr})^{0.75}\right]^{1/3} \tag{5}$$

where μ_m/μ_w is the viscosity ratio between the wall film and the average value in the main stream which in this case are considered equivalents, D/L is the ratio between the pipe diameter and the pipeline length, being negligible for long pipes, and **Gr** is the Grashof Number, $\mathbf{Gr} = D^3\rho^2 g\beta|\Delta T|/\mu_f^2$, where ΔT is the temperature differential between fluid and pipe wall. Equation 5 is valid only for $\mathbf{Gr}/\mathbf{Re}^2$ >1 when natural convection is more dominant than forced convection.

At the present analysis, the oil density ρ was considered as a function of pressure and temperature, being given by the following relation

$$\rho=\rho_{ref}\,[1-\beta\,(T-T_{ref}\,)]+(p-p_{ref}\,)/\,a^2 \tag{6}$$

where a and β are the speed of sound and the thermal expansion coefficient, respectively, both assumed constant, ρ_{ref} is the reference density evaluated at the reference pressure p_{ref} and reference temperature T_{ref}. The absolute viscosity μ_f and the thermal properties, such as specific heat at constant pressure c_p and thermal conductivity k were considered constant.

2.1 Model 1

In this approach U_e in Eq. 3 is the inner convective heat transfer h_{in}, and T_{ref} is T_{is}, the inner wall temperature which is determined by solving transient heat conduction equation, taking into account the thermal capacity of the materials. To simplify the problem, the axial diffusion is neglected, and at each axial location, the radial conduction equation is solved

$$\rho_i\ c_{pi}\,\frac{\partial T_i}{\partial t}=\frac{1}{r}\frac{\partial}{\partial r}\Big(r\ k_i\,\frac{\partial\, T_i}{\partial r}\Big) \qquad 1\le i\le N \tag{7}$$

where T_i is the wall layer temperature, ρ_i, c_{pi} and k_i are the density, heat capacity, and thermal conduction of the material, respectively and N is the number of layers, including the pipe wall. These thermal properties are considered constant and temperature independent. The boundary conditions at the inner and outer walls of the main pipe are:

$$-k_1\,\frac{\partial T_1}{\partial r}=h_{in}\,(T-T_{is}) \qquad ; \qquad -k_N\,\frac{\partial T_N}{\partial r}=h_o\,(T_{os}-T_\infty) \tag{8}$$

where h_{in} and h_o are, respectively, the inner and outer convective heat transfer coefficients, T_{is} is the inner wall temperature, T_{os} is the outer wall temperature, T_∞ is the ambient temperature, and r is the distance in the radial direction.

The outer convective heat transfer coefficient is independently calculated by correlations for forced convection over a pipe laying on the seafloor. At the present work the following correlation was employed (Knudsen and Katz, 1958)

$$\mathbf{Nu_o} = h_o D_o / k_\infty = 0.0266\, \mathbf{Pr}^{1/3}\, \mathbf{Re}_o{}^{0.805} \tag{9}$$

where D_0 is the outside pipe diameter, k_∞ the seawater thermal conductivity and $\mathbf{Re}_o$ the Reynolds Number based on seawater maximum bottom currents and the outside pipe diameter.

2.2 Model 2

The reference temperature T_{ref} for Model 2 is the ambient temperature T_∞. Model 2 is based on the overall heat transfer coefficient U_G (based on the inner diameter of the pipe), which is calculated ignoring the heat capacity of the pipeline:

$$\frac{q_{in}}{\Delta x} = h_{in}\, \pi\, D\,(T - T_{is}) = U_G\, \pi\, D\,(T_{is} - T_\infty) \quad ; \qquad U_G = \left[Res_{wall} + \sum_{i=1}^{N-1} Res_{layer,i} + Res_o \right]^{-1} \tag{10}$$

where, Res_{wall}, Res_{layer} and Res_o are the equivalent thermal resistance for the pipe wall, the insulating layers and outer wall to the ambient resistance, defined in the following way

$$Res_{wall} = \frac{D}{2k_1}\mathbf{ln}\left(\frac{D_e}{D}\right) \quad ; \quad Res_{layer,i} = \frac{D}{2k_i}\mathbf{ln}\left(\frac{D_{ei}}{D_i}\right) \quad ; \quad Res_o = \frac{D}{D_o}\frac{1}{h_o} \tag{11}$$

where D is the inner pipe diameter, D_e is the exterior diameter of the wall pipe. Each layer i has a thickness $e_i = D_{ei} - D_i$, where D_{ei} and D_i are the exterior and interior diameter of each insulating layer, respectively.

3. Numerical Model

The solution of the equation governing the flow field inside the pipeline was determined by a finite difference scheme, while the pipe wall temperature distribution was determined by a finite volume technique (Patankar, 1980). The contribution of the heat capacity to the pipe wall energy equation was included in the numerical code PIGSIM (Nieckele et al., 2001). The spatial derivatives are approximated by a central difference scheme, and a fully implicit approach is adopted for the time integration. In this code, a full thermal model is considered, in which the coupled continuity, linear momentum and energy equations are solved simultaneously inside the pipeline, employing a direct heptadiagonal algorithm. At each axial location the transient, radial conduction equation is solved along the pipeline wall (duct wall and insulation layers), by a tri-diagonal algorithm.

The software *TLNET* used in this study for comparison purposes determines the flow field by a simultaneous solution of the mass and momentum equations, discretized based on a four-point, implicit finite difference formulation scheme. The resultant set of equations has second order accuracy in space and first order in time. When the temperature distribution is needed, a separate set of equations is solved based on an implicit upwind finite difference scheme using a Gauss-Seidel iteration to solve for temperature variation at each time step, leading to a first order accuracy in time and space (Licenergy Inc, 2000).

STONER employs a uniform mesh and solves the linearized flow conservation equations at each time step, employing second order precision. The heat loss to the ambient is determined employing a methodology very similar to the Model 1 implemented in the present work. Simulations of the hydraulic responses of a pipeline carrying a single phase fluid are performed using a collocation procedure to solve the coupled system of partial differential equations (Luskin, 1979).

Although, the *OLGA* simulator was developed for the solution of multi-phase flow, at the present work, the flow was considered as having only one phase, in order to allow comparison with the different softwares, with regard to the influence of the thermal capacity. An implicit solution technique is utilized for the time integration of the conservation equations and an upwind differencing is used for the finite difference approximation of the space derivative, a LU matrix inversion routine (Peyret and Taylor, 1983) is then used to solve the system of equations.

4. Case studied

One of the purposes of the cool down analysis is to determine the time required for the flowline to attain a critical temperature after a shutdown. Therefore, the initial condition consisted of a steady state flow of oil. Cool down commenced once a valve at the entrance of the pipe was closed (Fig. 1). The study was performed on a 1 km pipeline with the parameters presented in Table 1. The fluid properties are listed in Table 2. For comparison, the case was simulated with the models described in section 2 and the commercial softwares *TLNET, STONER* and *OLGA*.

Figure 1. Pipeline configuration.

The initial condition was specified as the steady state flow and temperature distribution considering oil entering the pipeline at 60 °C, losing heat to the sea water at 5 °C, discharging to an ambient at atmospheric pressure and with a fully open valve at the entrance (Fig. 1). The transient regime began when the entrance valve was closed. It was considered that a critical temperature equal to 15 °C. The flow rate is determined from

$$Q = \alpha\,(Cd\;\;A_v)_o \sqrt{2\,(P_s - p)/\,\rho} \tag{12}$$

where, the fully open valve discharge coefficient, $(C_d\,A_v)_o$ was set equal to 0.1 m^2, with a reservoir pressure of p_s = 7.16 kgf/cm^2. α is the percentage of the valve opening. The resulting initial flow rate was equal to 0.05m^3/h. The entrance valve was closed in 30 seconds.

The seawater parameters utilized were: stream velocity of 1 m/s, density of 1025 kg/m^3, thermal conductivity of 0.59W/(m-K), viscosity of 1.08×10^{-3} Kg/(m-s) and **Pr** = 8.81, resulting in an outer heat transfer coefficient of 2000 W/(m^2-K) and an overall heat transfer coefficient U_G equal to 4.22 W/(m^2-K).

Table 1. Pipeline parameters.

	Thickness (mm)	Density (kg/m^3)	Thermal conductivity [W/(m-K)]	Heat capacity [J/(kg-K)]
Pipe (*D*= 6")	12.7	7800	50	500
Insulation	200	52	0.38	657

Table 2. Fluid properties (at reference conditions: *p*=1 kgf/cm^2, *T*=20 ºC)

Density (kg/m^3)	Speed of sound (m/s)	Thermal expansion coefficient (1/K)	Viscosity (cP)	Heat capacity [J/(kg-K)]	Thermal conductivity [W/(m-K)]
882.7	1286	7.880×10^{-4}	25.72	1.831×10^{3}	1.313×10^{-1}

To define the fluid properties for the *TLNET* software, tables must be prepared, with the bulk modulus ($K=\rho\, a^2$), coefficient of thermal expansion and heat capacity c_p coefficient at various temperatures and pressures. The program fits these data to an empirical equation of state. For maximum accuracy, the data should span the entire expected operating pressure and temperature ranges. Further, one must specify the density at a reference condition. The table was prepared so that the same fluid was defined in all softwares. The transient scenario was created by closing the same valve at the entrance of the pipeline, during the same 30s. *TLNET* does not consider the thermal capacity of the wall in the analysis.

Parameters used in the *OLGA* simulation are also defined in tabular format and they were analogous to the ones defined for *TLNET*. The software *OLGA* allows the simulation considering the thermal capacity of the material (option called *Olga-Wall*) and not considering it. The second option, called *Olga*-Ugiven uses an overall heat transfer coefficient.

The *Stoner Pipeline Studio* uses the Slightly Compressible Liquid (SCL) equation of state, Eq. (6), to describe the physical state of the fluid in the pipeline. The same properties shown in Table 1 and 2 were also defined.

The present problem is governed by a series of dimensionless parameters: (i) Geometric: D/L, e_w/D, e_{iso}/D; where *w* and *iso* refer to the pipe wall and insulating layer (ii) Properties: k_w/k; k_{iso}/k, α_w/α; α_{iso}/α, Pr, where α is the thermal diffusivity; (iii) Initial condition: Re=1.43×10^5, steady state flow and temperature distribution; (iv) Boundary conditions: internal and external dimensionless heat transfer coefficient, and ambient temperature.

To investigate the influence of the thermal capacity, initially a solution was obtained with Model 1 and Model 2 for the base case (Tables 1 and 2) and the results were compared with the commercial softwares solutions. Then, the initial condition, the boundary conditions, the fluid properties and pipe properties were kept constant and the influence of the insulation parameters was investigated. In all analyses, the simulation time was 12 hours. After a grid test, a 10s time step, and 10 m node spacing were defined, so that a temperature variation smaller than 1% was obtained. However, for the *TLNET* simulator, it was necessary to utilize a time step of 1 s and a node spacing of 5m, because of the lower accuracy of the discretization scheme. Only one control volume was specified at the pipe wall and 5 control volumes were utilized at the insulation layer.

Figure 2 shows the temperature variation with time in a section located in the middle of the pipe (500 m), obtained with the two models described here and with the three commercial softwares. In the same figure, the results obtained completely neglecting insulation for the pipeline resting on the seabed were also included. It can be observed that, if there was no insulation, the oil temperature would reach the critical temperature in less than 2 hours.

The solution obtained with Model 2, *TLNET* and *Olga*-Ugiven were all the same, since the thermal capacity of the pipe and insulating layers were neglected. They predicted a 6.5 hours period for the mid pipe temperature to reach the critical temperature. An analysis of Fig. 2 shows that the heat capacity of the pipe wall and insulation (Model 1) slows down the cool down process, increasing in more than five hours the time to reach 15^{o}C, in relation to the solution of Model 2, that neglects this contribution. The temperature profile obtained with *Stoner* is slightly higher than Model 1. The solution obtained with *Olga*-Wall is the least conservative of all, and after 12 hours the temperature is still high, around 27 ^{o}C. The temperature drop using the 3D Thermal module of the *OLGA* simulator is smaller than that predicted by the other simulators.

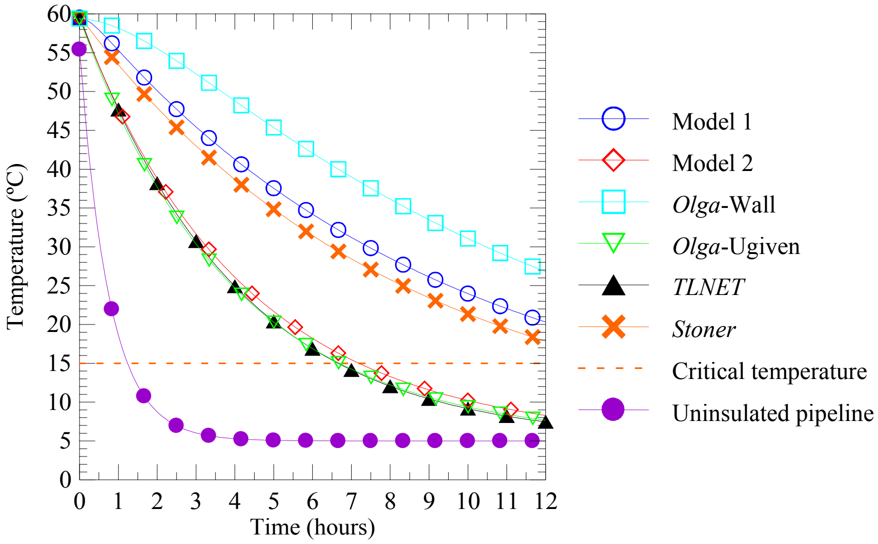

Figure 2. Temperature variation with time during cooldown at x = 500m.

Figure 3 shows the temperature drop along the pipeline length for two different time instants during the cooldown (4 and 8 hours after closing the entrance valve). Analyzing the axial temperature distribution in Figs. 3a and 3b, it can be seen that all models predicted a very small temperature drop along the pipeline. The results obtained using *TLNET*, Model 2 and *Olga*-Ugiven were once again almost coincident. It can also be seen that, as already mentioned, the software *OLGA* predicted a slower cooldown than all others models. As shown in Fig. 2, the results obtained with Model 1 were similar to the ones obtained with *Stoner*. It should be mentioned here, that after a very long time interval, all softwares predict the same temperature distribution, i.e., equal to the sea water temperature, T_∞.

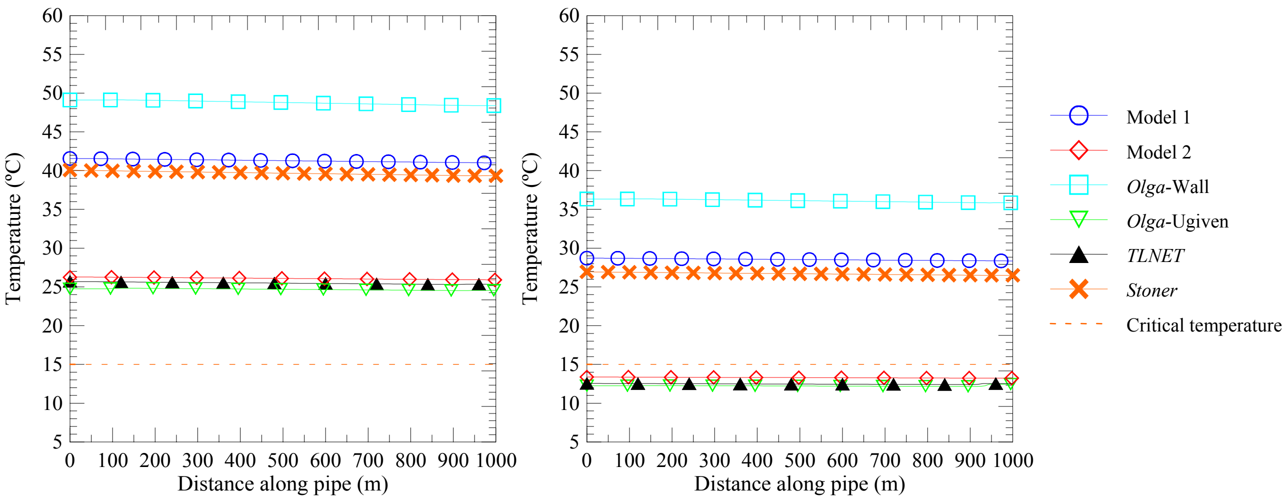

(a) 4 hours after shutdown (b) 8 hours after shutdown

Figure 3. Temperature profile along pipeline, during cooldown.

The main difference from Model 1 and *OLGA*, is that at the present model the axial diffusion is neglected, while *OLGA* considers the heat conduction at the pipe wall and insulation in both spatial directions (radial and axial). However, the nearly uniform axial temperature distribution justifies the approximation of neglecting the axial diffusion. Therefore, the slower cooldown time predicted by *OLGA* cannot be explained by the fact that this software accounts for the axial diffusion. The influence of the internal heat transfer coefficient was investigated and it was verified that it significantly affects the temperature distribution. Therefore, the heat transfer correlation employed by *OLGA* and not informed in the manual could be responsible for the differences.

The influence of the insulation parameters can be appreciated in Figs. 4 and 5, where the solution was obtained with Model 1 and 2, maintaining the same fluid, pipeline, initial and boundary condition, and varying the insulation parameters. The reference parameters for the base case are: k_{iso}/k =2.89 and α_{iso}/α= 136. For the first test, shown in Fig. 4, the thermal diffusivity α was kept constant and the conductivity k was varied. The reference value was divided and multiplied by 10. The results in Fig. 5 were obtained varying the thermal diffusivity α, while maintaining the same k. The thermal diffusivity of the insulation was divided by 20, it was also multiplied by a very large number.

It can be seen in Fig. 4 that, as expected, there is a smaller temperature drop, when the conductivity decreases. The influence the thermal capacity ($\rho\, c_p$) can be observed at Fig. 5, where a smaller temperature drop can also be observed when α decreases. In Fig. 4, k was varied, maintaining α constant, therefore, $\rho\, c_p$ were also varied. Since α is the ratio of these two quantities, and both have the same influence on the temperature, there is an optimum value of k for a given α, as one can see by the reduction of the influence of the stored energy as k increases and decrease from the reference case.

Figure 5 illustrates the effect of the thermal diffusivity on the temperature variation with time at x= 500 m. The reference α was divided by 20, and since the temperature variation was small with larger α values, a very large value (equivalent to zero $\rho\, c_p$) was specified. At the same graft, one can also observe the result obtained with Model 2, which employs the overall heat transfer coefficient and it is independent of α (since it neglects the thermal capacity of the pipe and insulation). An additional curve was also included corresponding to zero thermal capacity not only for the insulation, but also for the pipe. It is interesting to observe that since the thermal capacity of the insulation is already small, neglecting it does not influence the temperature distribution. Surprisingly, the influence of the thermal capacity of the pipe wall is significant, even though its thickness is small. At the mid section of the pipe, a temperature difference of 10 ^{o}C can be observed after 12 hours of cooling, due to the thermal capacity of the pipe wall.

Still analyzing Fig. 5, one can compare the prediction obtained with Model 2, which employs a steady state over-all heat transfer coefficient and the prediction of Model 1, neglecting the thermal capacity of the pipe and insulation. It can be observed that the solution obtained neglecting the thermal capacity of the pipe wall and insulation (α_{iso}/α=α_w/α=∞) and the Model 2 prediction are relatively similar, however the models predict a temperature distribution with a difference of approximately 2 ^{o}C. These curves should coincide and the difference can be attributed to the radial mesh distribution employed, since the mesh was refined in the radial direction and the difference was reduced.

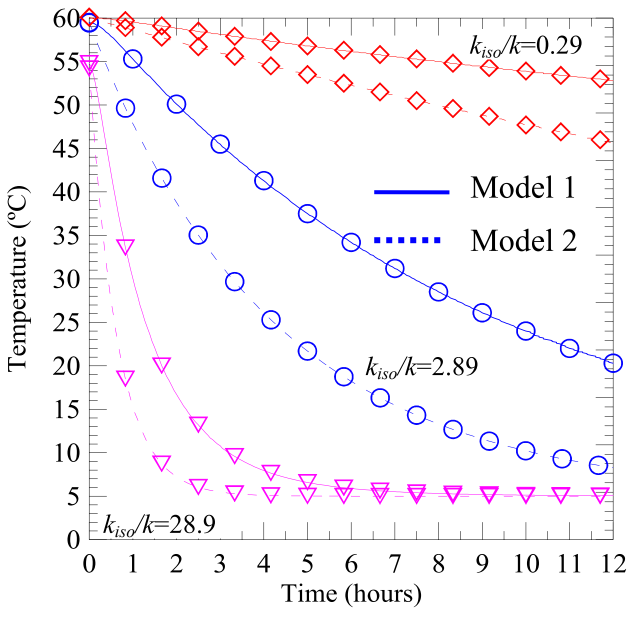

Figure 4. Temperature variation with time at x = 500m. Influence of the insulation thermal conductivity.

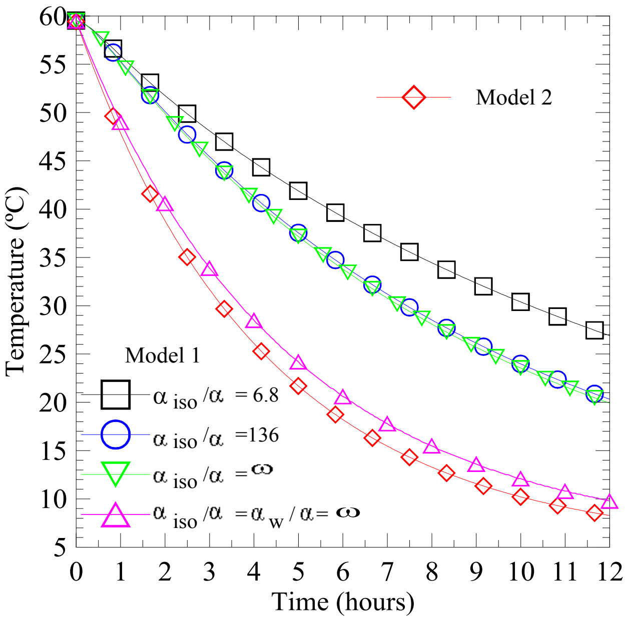

Figure 5. Temperature variation with time at x = 500m. Influence of the insulation thermal diffusivity.

5. Final Remarks

A transient thermal model has been developed to solve the temperature distribution within the wall of a pipeline. The thermal performance of insulated pipelines was investigated, considering both a detailed model for the temperature distribution within the wall and using an overall heat transfer coefficient ignoring the thermal capacity of the wall.

Observations show that a smaller temperature drop is obtained when the energy stored at the pipe wall and insulation is considered. These results illustrate the importance of accounting for the transient thermal properties in the cooldown calculations. As a conclusion, it can be stated that it is essential to account for the thermal capacity of the wall layers that compose the pipeline, since they significantly influence the cooldown time.

The relative influence of the insulation with the type of fluid and different operation situation remains to be evaluated. However, even though a simple test was performed, it is already clear that it is essential to address correctly the stored energy at the insulation and pipe wall, and the use of a steady state overall heat transfer coefficient must be avoided.

6. Acknowledgement

The authors thank CNPq and CAPES for the support during the development of this work.

7. References

Brown, S.T., Clapham, J., Danielson, T.J., Harris, R.G., Erickson, D.D., 1996, “Application Of A Transient Heat Transfer Model For Bundled, Multiphase Pipelines”, PE 36610, SPE Annual Technical Conference.

Cerqueira, D.L. Su, J. and Stefen, S., 2004, “Simulation of Transient Heat Transfer of Sandwich Pipes with Active Electrical Heating”, OMAE 2004, paper no. 51233.

Chiu, K. and Thakur, S.C., 1991, “Modeling of Wellbore Heat Losses in Directional Wells Under Changing Injection Conditions”, 1991 SPE Annual Fall Meeting, Dallas, paper SPE 22870, pp 517 – 528.

Danielson, T.J., Brown, L.D., 1999, “An Analytic Model For A Flowing Bundle System”, SPE 56719, SPE Annual Technical Conference.

Denniel, S., Blair, C., 2004, “Aerogel Insulation For Deepwater Reelable Pipe-in-Pipe”, OTC 2004, paper 16505.

Dwight J., Nigel M., Janardhan D., 2004, “Prediction of cool down times and designing of insulation for subsea production equipment”, OTC 16507

Fox, R. W. and McDonald, A. T., 2001, “Introdução à Mecânica dos Fluidos”, Livros Técnicos e Científicos Editora.

Holman J.P., “Transfêrencia de Calor”, McGraw-Hill.

Incropera P., DeWitt P., 1990, “Introduction to Heat Transfer”, John Wiley & Sons, Second Edition.

Knudsen J.G., Katz D.L., 1958, “Fluid Dynamics and Heat Transer”, McGraw Hill Book Co.

Licenergy Inc., 2000, “Pipeline Studio User’s Guide”.

Loch, K, 2000, “Flowline Burial: An Economic Alternative to Pipe-in-Pipe”, OTC 2000, paper 12034.

Luskin, M., 1979, “An Approximation Procedure for Nonsymmetric, Nonlinear Hyperbolic Systems with Integral Boundary Conditions”, SIAM J. on Numerical Analysis 16 pp. 145-164.

Nieckele, A.O., Azevedo, L.F.A., Braga, A.M.B., 2001, “Transient Pig Motion Through Pipelines”, Journal of Energy Resources Technology of ASME, Vol. 123, pp.260-269.

Patankar, 1980, “Numerical Heat Transfer and Fluid Flow”, Hemisphere Publishing Corporation.

Peyret, R. and Taylor, T. D. , 1983, “Computational Methods for Fluid Flow”, Springer-Verlag.

Wylie & Streeter, 1978, "Compressible Flow in Pipes", McGraw Hill

Zabaras, G.J.; Zhang J.J., 1998, “Bundle-Flowline Thermal analysis”, SPE 52632, SPE Annual Technical Conference.

8. Responsibility notice

The authors are the only responsible for the printed material included in this paper.